Supplementary Methods and Information for "Phase-locking and multiple oscillating attractors for the coupled mammalian clock and cell cycle"

Celine Feillet*[1], Peter Krusche*[2], Filippo Tamanini*[3], Roel C. Janssens[3], Mike J. Downey[2], Patrick Martin[1], Michèle Teboul[1], Shoko Saito[3,4], Francis Levi[5], Till Bretschneider[2], Gijsbertus T.J. van der Horst[3], Franck Delaunay[1], David A. Rand[2]

*** these authors contributed equally**

Corresponding authors: David Rand d.a.rand@warwick.ac.uk, Franck Delaunay mailto:**delaunay@unice.fr, Gijsbertus van der Horst g.vanderhorst@erasmusmc.nl**

[1] **Université Nice Sophia Antipolis, CNRS, INSERM, Institut de Biologie Valrose, Nice, France**

[2] **Systems Biology Centre, University of Warwick, Coventry, CV4 7AL, UK**

[3] **Department of Genetics, Erasmus University Medical Center, Rotterdam, The Netherlands**

[4] **present address: Department of Infection Biology, Faculty of Medicine, University of Tsukuba, Tsukuba, Japan**

[5] **INSERM, UMRS776 "Rythmes biologiques et cancers", Paul Brousse Hospital, Villejuif, France**

METHODS

1. Cell Biology.

1.1 Cell lines and reporters.

Circadian clock reporter cell line: NIH3T3 bearing the stably inserted Rev-erbα::Venus construct were obtained from Ueli Schibler[1] .

Cell Cycle reporter system: The Fluorescent Ubiquitination-based Cell Cycle Indicator (FUCCI) reporter system, which consists in a set of two fluorescent probes fused to either Cdt1 or Geminin, two cell cycle proteins which accumulate reciprocally during the G1 and S/G2/M phases respectively, has been described in Sakaue-Sawano et al., [2]. Based on this system, we designed a polycistronic retroviral vector that allows stable expression of the FUCCI reporter in a single vector (see below) in order to achieve a better stoichiometry of the

system. This construction includes the Cdt1 and Geminin sequences coding for G1 and S/G2/M probes respectively, fused to fluorescent reporters. They are separated by a 2A sequence to allow post-translational cleavage[3] and followed by a puromicin resistance cassette for subsequent selection (Supplementary Fig. S1a). The 2A-like sequences consist in a 19 amino acid region harbouring a self-processing activity mediating the co-translational cleavage of viral polyproteins[4]. This new FUCCI reporter was named “FUCCI-2A”.

1.2 Generation of FUCCI-2A transfer plasmid (pPRIPu CrUCCI)

The sequence encompassing the Geminin-T2Apeptide-mKO2-hCdt1 was synthesized by Epoch Biolabs, INC. (1306 FM1092 Rd, Ste 407 Missouri city, TX 77459-1565 http://www.EpochBiolabs.com) and cloned into a modified pBSK.

The amino acid sequences of the Geminin, mKO2, and hCdt1 are identical to those described in Sakaue-Sawano et al.,[2].

The 2A Amino Acid sequence (T2A) is that of the Thosea asigna virus (Sequence ID: gb|AAC97195.1)

Silent mutations were introduced to facilitate insertion in our retroviral vectors.

The pPRIPu CrUCCI used in this study (Supplementary Fig. S1b) was constructed as follow: the AgeI-SspI (in lowercase above) fragment from pBSK FUCCI was inserted in the pPRIPu HAa[5] digested with NgoMIV and HinCII. Additionaly, as mAG fluorescence wavelength was not compatible with that of Venus, we replaced the mAG marker with a E2-Crimson fluorescence in our final system (sequence provided on demand). Restriction map is reported in Supplementary Fig. S1b. The integrity of the entire FUCCI-2A sequence in the latter has been confirmed by sequencing analysis.

1.3. Stable cell line generation

Replication-defective, self-inactivating retroviral constructs were used for establishing stable NIH3T3_Rev::Venus_FUCCI-2A cell line. On day 1, HEK293T were seeded in 100 mm plates (1-2.10^6 cells per plate). On day 2, cells were co-transfected with 10 µg transfer (pPRIPu CrUCCI), 5 µg packaging (pCMV-gag-pol) and 5 µg envelope (pCMV-env-VSV-G) plasmids, using a Calcium Phosphate method. After 16 hours, medium was replaced with 5 ml fresh medium (day 3). Supernatant was harvested 48h after transfection and filtered on 0.45µm PES filters to remove cell debris. NIH3T3_Rev::Venus cells seeded at 10% confluence the day before were directly infected by applying filtered supernatant + 4 µg/ml polybrene (Sigma-Aldrich) to the cells (day 4). Medium was then added to transfected HEK cells for a second round of harvesting/infection the next day, following the same protocol (day 5). Viruses were left for 3 days before splitting infected cells and adding puromycin (4µg/ml) for selection. Cells were frozen 15 days later or used in subsequent experiments.

The resulting cell line stably expressed the following markers: Reverbα::Venus as a clock marker, mKO2::Cdt1 and E2-Crimson::Geminin as G1 and S/G2/M cell cycle phases markers respectively.

1.4 Flow cytometry

To ensure that the cell cycle was not perturbed by insertion of the transgene in NIH3T3_Rev::Venus_FUCCI-2A cells, as well as to validate this modified system as an accurate cell cycle reporter, we analysed the DNA content of proliferating cells using a Fluorescence-Activated Cell Sorter (FACS). NIH3T3_Rev::Venus_FUCCI-2A cells were seeded in 100 mm plates (1.10^6 cells per plate) and left to proliferate for 48 hours before cell analysis. Cells were resuspended and incubated for 30 min in Cytofix (BD Bioscience). After centrifugation, fixed cells were resuspended in PBS containing 0.1% Triton, 20 µg/ml RNAse A and 2 µg/ml Hoechst 33342 solution (Invitrogen) After a 10 min incubation, cells were harvested and analyzed using a BD LSR Fortessa (Becton Dickinson). mKO2, E2-Crimson and Hoechst were excited with a 561nm, 633 nm and 355 nm laser line, respectively. Fluorescence signals were collected at 586 nm (586/15 BP) for mKO2, at 670 nm (670/14) for E2-Crimson, and at 450 nm (450/40) for Hoechst 33342. The data were analyzed using the DIVA software (BD). Results shown in Supplementary Fig. S1c indicate that mKO2(+)E2-Crimson(-), mKO2(+)E2-Crimson(+), mKO2(-)E2-Crimson(+) cells populations had a DNA content consistent with their predicted phase of the cell cycle.

1.5 Time-lapse imaging

For recording, cells were seeded at 7-10% confluence (10^5 cells per well) in a 6 wells plate (Falcon), with white DMEM medium (high glucose) containing 1% Penicillin/Streptomycin, 10 mM HEPES and either 10%,15% or 20% FBS. Cells were left undisturbed for 48 hours. For the Dex-pulse condition, cells were incubated for 2 hours in the same medium as above, supplemented with 100 nM Dexamethasone (Dex). Cells were then returned to Dex-free regular medium just before recording. For recording, cells were placed in a Zeiss Axiovert 200M microscope (Zeiss) with a 10X Ph objective. A culture chamber, temperature and CO_2 controller (Pecon) were used to ensure constant suitable conditions for long term recording of the cells. Images were recorded every 15 minutes for 72 hours, using a Coolsnap HQ/Andor Neo sCMOS camera. Cells were briefly illuminated with a fluoarc HBO lamp (Zeiss) at reduced intensity and epifluorescence signals were recorded as follows: Venus: 1000 ms (filter cube: Ex 475/40 – Di 500 – Em 530/50), mKO2: 300 ms (filter cube: Ex 534/20 – Di 552 – Em 572/38), E2Crimson: 800 ms (filter cube: Ex 600/37 - Di 650 - LP 664).

A brightfield image for each frame was also acquired to ease cell tracking and analysis. Timelapse acquisition was controlled using a Metamorph 6.1/7.7 software.

1.6 Cell sorting

NIH3T3_Rev::Venus_FUCCI-2A cells were seeded in 100 mm plates (1.10^6 cells per plate) and left to proliferate for 48 hours before cell sorting. On the day of sorting, cells were trypsinized and resuspended in 1 ml PBS + 5% FBS + 2 mM EDTA. Based on their fluorescence, single cells were sorted as follows, using a BD FACS ARIA (Becton Dickinson): Non-marked: Early G1, mKO2 only: G1, mKO2 + E2-Crimson: Early S, E2-Crimson only: S/G2/M. mKO2 and E2-Crimson were excited with 561 nm and 633 nm laser lines, respectively. Fluorescence signals were collected at 610 nm (610/20 BP) for mKO2 and at 670 nm (670/14 BP) for E2-Crimson. A plate of non-sorted cells was used as control. The experiment was done in triplicate.

After centrifugation, cells were processed for total RNA extraction with NucleoSpin RNA II kit (Macherey-Nagel) according to manufacturer's protocol. RNA was kept at -80°C until use.

1.7 qRT-PCR

Quantitative RT-PCR. Measurements were performed with a Light Cycler 1.5 (Roche Applied Science) using SYBR green I dye detection according to the manufacturer's recommendations. cDNA, synthesized from 2-5 µg of total RNA using random primers and Superscript II (Invitrogen), was added to a reaction mixture (Faststart DNA SYBR Green I) with appropriate primers at 0.5 µM each: *Rev-erbα*: forward 5'-AACCTCCAGTTTGTGTCAAGGT-3' and reverse 5'-GATGACGATGATGCAGAAGAAG-3' (Supplementary Figure S1d); *Ccna2*: forward 5'-AAGACTCGACGGGTTGCTC-3' and reverse 5'-CCAGGGCATCTTCACACTCT-3' (Supplementary Figure S1e); *Ccne2*: forward, 5'- GCATCAGTATGAGATTAGGAATTG-3' and reverse 5'-CAGAATGCAGAACTTGAAAATGT-3' (Supplementary Figure S1f); *36B4*: forward 5'-GCTGATGGGCAAGAACACCA-3' and reverse 5'-CCCAAAGCCTGGAAGAAGGA-3';. Relative mRNA abundance was calculated using a standard curve method. Expression levels were normalized to the levels of the constitutively expressed *36B4* ribosomal protein mRNA.

2. Image and timeseries analysis

2.1 Cell tracking. Tracking cells using LineageTracker is a semi-automated process[6]. The input to LineageTracker is a sequence of images which were captured every 15 or 30 minutes (see Table S1: Summary of Datasets). There are different approaches to the choice

of cells to track. If the cells are sparse in the last frames, cells should be chosen from the end of the movie, making it easier to pick cells which can be tracked for a long period of time. In other movies, choosing cells from the beginning works better because the density of cells increases drastically at the end of the movie. To be able to conclusively analyse the resulting timeseries, around 20-50 lineages should be tracked per movie (we also show a list of how many lineages we tracked in Supplementary Table S2: Tracked Cell Counts and Period Lengths). Note that any cell that was visible from beginning to end of the recording was considered as a "mother cell" and was tracked, i.e. cells were not selected before tracking. As an output, we get the numerical timeseries for each of the three markers, information about when divisions occurred, and also information about the parent and children of each cell in the lineage tree. The file format and plugin we used for this have been made available at https://github.com/pkrusche/lineagetracker.jsonexport. The output of the cell tracking procedure is further illustrated in Figure 1b-d.

2.2 Numerical time series Analysis

Clock Periodicity Analysis

Our analysis of the clock period serves two goals:

1. To classify cells and lineages w.r.t. rhythmicity.
2. To determine period lengths of circadian rhythms.

We use the spectrum resampling software package developed by Costa et al.[7] for a first analysis of periodicity. This software determines the stationary period length in a circadian timeseries and confidence intervals for it by means of bootstrap resampling. We obtain

- an optimal set of period lengths together with confidence bounds and variance information;
- a de-trended version of the input timeseries; and
- a nonlinear least-squares fit of a sinusoidal curve obtained using these period lengths.

We encountered a few difficulties when trying to get accurate period length estimates due to noise in our data. In Figure 1c, we see the clock trace for a cell, and some diagnostic information from the period length finding procedure:

1. We first de-trend the clock curve (shown normalized as black dots) using a strongly smoothed trend curve, which aims to remove oscillations that have a period length longer than the time interval that was observed. This trend is shown using a dotted black line. The de-trended result is shown in blue.
2. Since we only have a few clock peaks in most cells, we find these peaks before using a smoothed version of the input data (shown in yellow). We then estimate the period using the average distance D between these detected peaks. If less than two peaks are found, we discard the data (assuming that the tracked cell does not have a functioning

clock). We then run the period length estimation on the part of the time series, beginning at no more than time offset $-D/2$ before the first peak and ending at most at time offset $+D/2$ after the last peak. This region is highlighted as the area between the grey shading.

3. Finally, we classify cells as rhythmic or non-rhythmic. A basic requirement is that the cell has at least one clock peak within its lifetime (marked using a red rectangle). In order to extract phase information (see below), we will further increase this requirement to demanding at least two peaks, and we require the period length to be between 5 and 50 hours. Secondly, we use an rae-type value obtained from the confidence bounds $[P_{lower}, P_{upper}]$ returned from the spectrum resampling tool:

$$rae = (P_{upper} - P_{lower})/(2P_{mean})$$

If $rae < 0.25$, the confidence interval is less than twice as large as the estimated period, therefore we assume that the estimated period value is acceptable. Visually, the quality of the period estimate can be assessed by looking at the width of the peak in the period spectrum samples plot (also, several peaks may occur -- we require that the oscillatory component in the circadian range must clearly be the strongest). In Table S2: Tracked Cell Counts and Period Lengths, we show the distributions of period lengths both for the clock and for the cell cycle.

4. Using the period estimate P from spectrum resampling, we fit a sinusoid of the form $f(t) = a\ cos\left(\frac{2\pi t}{P}\right) + b\ sin\left(\frac{2\pi t}{P}\right)$ to the timeseries. We then filter out clock marker peaks which are not within a fixed distance of a peak for this sinusoid. This eliminates spurious peaks, and makes our automated clock phase estimation more reliable.

Cell Cycle Event Extraction

We analyse timeseries for the G1 and S/G2/M markers for each cell cycle (the time period from the start of the timeseries or a division to the next division). In each such period, we identify three turning points for each marker:

a) the point where the marker starts rising,
b) the peak,
c) the point where the marker has dropped below the basal level.

Turning points are identified using a piecewise-linear model: we attempt to find the best-fitting upward-triangle. From the turning points, we estimate the durations of cell cycle phases (G1 phase, and S/G2/M combined). Once we have traces for the FUCCI Markers as shown in our Figure 1c, we segment these traces into cell cycle intervals. A cell cycle interval

is defined as the time interval between two consecutive cell divisions (or the start/end of the time series for the first/last intervals).

For each marker trace, we determine a baselevel. This baselevel will be used later on to decide whether a marker's peak is sufficiently large. Given the timeseries values $TS = [M(t_1), M(t_2), M(t_3), \dots, M(t_n)]$, we estimate the baselevel as follows:

$$baselevel = max([\mathrm{quantile}(TS, 0.05), min(TS) + 0.5 \cdot \mathrm{std}(TS), 0]).$$

In each cell cycle interval, and for each marker, we identify the following three timepoints:

a) t_a : The time when the marker intensity starts increasing towards the peak

b) t_b : The peak of the marker

c) t_c : The time when the intensity has dropped below the baselevel.

The timepoints are identified by finding the best fit for the following piecewise-linear model.

$$Model(t) = \begin{cases} c_1 & \text{if} \quad t < t_a \\ c_2 t + c_3 & \text{if} \quad t + a \le t < t_b \\ c_4 t + c_5 & \text{if} \quad t + b \le t < t_c \\ c_6 & \text{otherwise.} \end{cases}$$

We choose values for $c_1, c_2, c_3, c_4, c_5, c_6$ which minimise the squared error:

$$\mathrm{SE} = \sum_{i=1}^{n} (Model(t_i) - M(t_i))^2.$$

In order to accept the fit, we require:

- Condition 1: The height of the peak must be above the baselevel: $Model(t_b) > baselevel$.
- Condition 2: Model values after t_c must be below the baselevel: $Model(t > t_c) < baselevel$ (we allow exceptions for the G1 marker in order to identify G1 arrest).

We obtain the six values of $t_a^{G_1}, t_b^{G_1}, t_c^{G_1}, t_a^{SG_2M}, t_b^{SG_2M}, t_c^{SG_2M}$. In order to proceed, we require that $t_b^{G_1} < t_b^{SG_2M}$, i.e. that the G1 peak must occur before the S/G2/M peak.

The time of the G1-S transition is estimated as follows.

$$t_{G_1-S} = \begin{cases} t_b^{G_1} & \text{if only the G1 fit was succesful,} \\ t_a^{SG_2M} & \text{if only the SG2M fit was successful,} \\ \mathrm{mean}(t_b^{G_1}, t_a^{SG_2M}) & \text{if fits for both series were successful,} \\ undefined & \text{otherwise.} \end{cases}$$

This way, we can use the two markers for redundancy in cases where it is not possible to find a good fit for the timeseries data on both the G1 and S/G2/M traces.

In Table S3: Data Quality for Analysed Cell Cycle Intervals and Clock, we show success rates for extracting G1-S transition times using this method. In general, we appear to be able to extract data for more than 50% of all cell cycle intervals. However, this includes intervals at the beginning or end of the timeseries – these are not useful for our analysis since we cannot know the exact length of the corresponding cell cycle which starts/ends outside of the

observed time interval. When restricting attention to only fully observed cell cycle intervals, the accuracy of our method increases to close to 100% in most datasets (in Table S3, the first success rate relates to fully observed cell cycles, the second one to all intervals in the dataset). Moreover, the success rate increases when we restrict our attention to cells with a functioning clock.

2.3 Circadian Phase-timing of Cell Cycle Events

Clock Phase. In order to establish whether there is a correlation between the clock and cell division timing, we calculated estimated clock phase values for each recorded time point. We consider two different methods for estimating this phase value.

Since the circadian clock is a cyclic process, we consider clock phases from the interval $[0,2\pi)$. We assign phase 0 or 2π to the time at which the clock marker peaks. This way, we can associate a phase angle $\varphi_{cl}(t)$ with each time-point. We use the following methods for estimating $\varphi_{cl}(t)$ (see also Figure 1c, top part):

1. We use the fitted sinusoid obtained using the period estimate from spectrum resampling. This fit gives us a direct estimate for the phase angle. Assuming that we have obtained a fit

$$f(t) = a\,cos\left(\frac{2\pi t}{P}\right) + b\,sin\left(\frac{2\pi t}{P}\right),$$

we can obtain a phase angle $\varphi_{cl}(0) = arctan(b/a)$, and we subsequently set

$$\varphi_{cl}(t) = \varphi_{cl}(0) + \frac{2\pi \cdot t}{P}.$$

A drawback of this method is that estimates for $\varphi_{cl}(t)$ will not be accurate if the period of the clock marker changes over time, since we assume that the period length P is constant. An advantage is that we can estimate phase angles for the entire time interval we used for determining the period length by spectrum resampling.

2. Using the peaks from our peak-finding procedure, we can interpolate the values of φ_{cl} from peak to peak. Assuming we have detected a peak in the Rev::VENUS marker at times $t_1, t_2, \dots, t_N$, we can estimate φ_{cl} as follows.

$$\varphi_{cl}(t) = \begin{cases} \frac{2\pi}{P}\frac{t - t_i}{t_{i+1} - t_i} & \text{If } t \text{ is inside the interval } [t_i, t_{i+1}) \\ undefined & \text{otherwise.} \end{cases}$$

A drawback of this model is that we can only estimate phases in time intervals between two clock peaks (i.e. we cannot estimate the clock phase at the beginning and at the end of the time series).

Random Background Model

We would like to distinguish the distribution of the estimated phases of cell cycle events (cell division or G1-S transition) from a random background model. For this, we assume that in the case of no correlation between the events and the clock, any observed phase would be equally likely to be associated with some cell cycle event (Supplementary Fig S2b-c; grey shaded histogram and area).

For a given dataset of cells, let $\{\mathrm{Clock}(t_1, C), \ldots, \mathrm{Clock}(t_{N(C)}, C)\}$ be all recorded clock marker values for all distinct cell cycles $C \in 1 \ldots Number\ of\ observed\ cell\ cycle\ intervals$. We can also associate a phase angle $\varphi(t_k, C)$ with each time t_k and cell cycle interval C. We collect all these phase angles for an experiment into a set $B = \{\varphi(t_k, C)\ with\ k = 1 \ldots N(C)\ and\ C = 1 \ldots Number\ of\ observed\ cell\ cycle\ intervals\}$. If a class of events like cell divisions or G1-S transitions is not associated with a specific set of clock phases, the observed phases for this class of events should be a uniform random sample of all phases in set B (assuming all our phase estimates are taken at equally spaced time intervals).

Considering all division (or G1-S transition) events in a dataset, we compare the distribution of $\{\varphi(t, C) \mid \text{Event at } t \text{ in interval } C\}$ to the distribution of events obtained from drawing E values uniformly at random from all observed phase values in set B defined above. We perform this comparison using two different methods:

- We can compare the cumulative distributions, either visually (omitted due to space constraints), or using an appropriate statistical test. We compare cumulative distributions using the two-sample Kolmogorov-Smirnov test[8], or the Kuiper test for circular distributions[9]. We test for:

  $$\begin{cases} H_0 & = \text{Distribution of phases cannot be distinguished from random background.} \\ H_1 & = \text{Distribution of phases is different from background.} \end{cases}$$

  H_0 corresponds to the case where either cell divisions or G1-S transitions happen independently of the clock phase. In Table S4: Cell Cycle Event Analysis, and background vs. phase distribution test p-values, we give p-values for accepting/rejecting H_0.
- Using bootstrap sampling and kernel density estimation[10, 11], we can compare the phase histograms directly (see Supplementary Fig S2 b-c ; yellow and red histograms).

2.4 Population-level Analysis

Plots of Population-based Event Densities over Time

To check if our tracked cells were synchronised on a population level, we created density plots and histograms for all cells in our tracked population, showing whether there are

preferred times during the experiment when cells like to divide (Supplementary Fig S2e), or have their clock marker peaks (Supplementary Fig S2d). We expect the Dexamethasone-treated cells to have synchronised clock marker peaks (since the treatment will reset the clock in all cells before the experiment). In the unsynchronised cells, we expect an irregular behaviour since most cells will not be phase-synchronised.

Clock Phase vs. Cell Cycle Phase

To study the phase coupling in our cell populations, we may first assume that the cells are in a steady state, and estimate a phase diagram for their trajectories. To do this, we will need to define a cell cycle phase similar to the way we defined a clock phase above:

$$\varphi_{cc}(t) = \begin{cases} 0 \dots \pi & \text{from birth to G1} - \text{S transition,} \\ \pi \dots 2\pi & \text{from the G1} - \text{S transition to cell division.} \end{cases}$$

Each cell that is observed at time t then has a location $(\varphi_{cl}(t), \varphi_{cc}(t))$. Both φ_{cl} and φ_{cc} are cyclic coordinates (they wrap around at 2π). Therefore, the movement of the cells in their $(\varphi_{cl}(t), \varphi_{cc}(t))$ coordinates can be visualised by a point moving on the surface of a torus.

Our dataset allows us at each time t to estimate the location $(\varphi_{cl}(t), \varphi_{cc}(t))$ and speed $(\dot{\varphi}_{cl}(t), \dot{\varphi}_{cc}(t))$ for all cells. Given locations and speeds of all observed cells, at each time point, we can use two dimensional kernel density estimation[12] to estimate the average speed of movement $(\dot{\varphi}_{cl}, \dot{\varphi}_{cc})$ on a regularly-spaced grid along the surface of the torus. The result is a streamline plot. Underlaid under the streamline plot, we show estimated cell densities over the course of the experiment for each location on the torus (Figure 2d). For the unsynchronised populations (fbs_10 and fbs_15), we can see that the cells prefer to move along a common set of trajectories on the torus surface (Figure 2d).

Analysis of the Dynamic Behaviour

In order to better understand whether there is a transient behaviour caused by the Dexamethasone treatment at the beginning of the experiment, we have derived two methods which allow us to analyse and visualise the dynamics of how clock and cell cycle are connected.

Timelapse of Clock and Cell Cycle Phase Progression

A first method to visualise the dynamic coupled behaviour of clock and cell cycle is to visualise the progression of clock and cell cycle phases over time in a movie with a frame for each time point t. In each frame, we plot $\varphi_{cl}(t)$ against $\varphi_{cc}(t)$ for all cells. The resulting movie (see Supplementary movies 2 and 3) reveals the following types of behaviour:

1. In the unsynchronized populations, we see that cells independently follow a main direction of movement along a preferred path. Some cells may skip between the main

trajectories and re-join when they meet the main path in the next cycle (Supplementary movie 2).

2. In the Dexamethasone-synchronised populations, we can see whether cells divide in groups (and at which phase). In the movies, we have coloured the cells according to the peaks in the divisions/time density histograms (Supplementary Movie 3).

Clustering of Division Phases over Time

Another way to visualise the phase dynamics of cell divisions is to create a 2-dimensional scatter plot of division clock phases over time. The resulting plots are shown in Supplementary Figure S3, S4 and S5.

The main idea of our clustering approaches is to:

- establish whether cell divisions occur in groups over the time of the experiments,
- relate these groups to a period ratio obtained by dividing the clock period by the cell cycle time for each cell cycle interval.

These complementary approaches reveal more information than only looking at the density of division events over time or clock phase individually, and have allowed us to better understand and visualise how the clock and the cell cycle are coupled in a non-trivial fashion.

To implement our analysis, we use the R package 'MClust'[13]. MClust is an R package for model-based clustering, classification, and density estimation based on finite normal mixture modelling. This approach is more general than the method used by Nagoshi et al.[1], who use a similar method to show that their distribution of observed cell division phases has three peaks.

We use two approaches:

Clustering method 1. We plot a data point for each cell division. For the x-axis, we show the experiment time of the division, and on the y-axis, we show the estimated clock phase at this time. We cluster the resulting set of points in two dimensions using Mclust as follows.

- Each cell cycle interval for which we observe a division and which we can associate with two clock peaks adds a data point $(t_i, 24\frac{\phi_{cl,i}}{2\pi})$ to our dataset (since Mclust uses an Euclidean distance, we scale the clock phases to lie within an interval of [0, 24)).
- Since the clock phase 'wraps around' at 2π, we create a copy of each data point $(t_i, \hat{\phi}_{cl,i})$ at $\left(t_i, \hat{\phi}_{cl,i} + 2\pi\right)$ and $(t_i, \hat{\phi}_{cl,i} - 2\pi)$ as illustrated by the following R code:

```
# Assume dataframe data contains two columns, t in column 1
# and phi_cl in column 2

# short range cyclic: append a fraction
# of the data again on the top and bottom
cyclicdata <- rbind(data,
                    cbind(data[,1], data[,2] + 2*pi),
                    cbind(data[,1], data[,2] - 2*pi))
cyclicdata <- cyclicdata[
     (cyclicdata[,2] >= -overlap) &
```

```
     (cyclicdata[,2] < 2*pi+overlap),]
# Scale phases to 0-24
cyclicdata <- cbind(cyclicdata[,1], cyclicdata[,2]/2/pi*24)
```

- We run Mclust to obtain a 2-D clustering / mixture distribution for all points in the dataset constructed above.

```
cdata <- Mclust(cyclicdata, G=1:ncl, modelnames="VVV")
```

- After we have run Mclust, we merge clusters which overlap by containing copies of the same datapoints as shown above:

```
#' compute pairwise half-torus distance (0-24 wrapping y coordinates)
halftorusdist <- function(p1, p2) {
  p1y = p1[2] %/% 24
  p2y = p2[2] %/% 24
  p2d <- min(abs(p1y-p2y), 24-abs(p1y-p2y))
  return (sqrt((p1[1]-p2[1])^2 + p2d^2))
}

#' Pairwise distances for classification centroids
pairwiseclassdists <- function(cyclicdata, cdata) {
  dists = matrix(nrow=cdata$G, ncol=cdata$G)
  for(i in 1:cdata$G) {
    ci = c(mean(cyclicdata[cdata$classification == i, 1]),
           mean(cyclicdata[cdata$classification == i, 2]))
    for(j in i:cdata$G) {
      cj = c(mean(cyclicdata[cdata$classification == j, 1]),
             mean(cyclicdata[cdata$classification == j, 2]))
      dists[i,j] = halftorusdist(ci,cj)
    }
  }
  return(dists)
}

#' merge clusters with centroids closer than threshold
mergedclusters <- function(classification, dists, threshold) {
  newclass = classification
  for(i in 1:nrow(dists)) {
    for(j in i:nrow(dists)) {
      if(dists[i,j] < threshold) {
        newclass[newclass == j] = i
      }
    }
  }
  return(newclass)
}

dists <- pairwiseclassdists(cyclicdata, cdata)
classes <- mergedclusters(cdata$classification, dists, 2)
data$classification <- classes[1:nrow(data)]
```

- Each division produces two child cells. If one or both of these cells divide again, we can determine the cluster in which this division happens. The result of this analysis can be visualised in two different ways:
    - We can draw arrows between the division data point of each mother cell and the division data points of its two children.
    - We can aggregate the information above by connecting the clusters. We show the relative number of children dividing in each subsequent cluster by varying the thickness of the arrow (see Supplementary Figure S4 and S5, first two plots for each dataset).
- We split our lineages into groups depending on which cluster the last divisions in each lineage occur in. This is possible because cells divisions within each lineage mostly fall into the same clusters.

While Nagoshi et al.[1] reported a three-peak distribution compatible with ours it is not possible from the results reported in their paper to tell whether their data contains cells of both of the two types that we find. We believe it is likely that the behaviour seen by Nagoshi et al.[1] (three peaks in the phase histogram over the entire time of the experiment) is the result of the way in which the subset of peaks in the 2-D density of clock phase at cell division over time overlap. To illustrate this, we show phase histograms for clock phase at cell division for each cluster obtained above separately (see Figure S3, S4, S5, rightmost plot in the top row for each dataset). Moreover, in our experiments with 20% FBS (see Supplementary Figure S4b), we see that the children coming out of the first cluster of divisions are divided into two groups: one group which divides again at a mean phase of around π (cells which divide first in the red cluster and their children dividing in the blue, and then the purple cluster), and another group of cells which divides at phases around $\pi/2$ (dark yellow/olive green cluster) and $3\pi/2$ (green cluster). When plotting the division clock phase histograms for both groups, we get two distinct behaviours, one that corresponds to 1:1 locking, and another one that corresponds to 3:2 phase-locked behaviour. In our analysis (see Figure 4b), differently from the figure shown by Nagoshi et al.[1], the three peaks of the division phases are not of equal size. This is explained by the fact that our data includes all children in each lineage that we were able to track (it is our understanding that Nagoshi et al.[1] only tracked one cell per lineage). Therefore, the first peak will be the smallest, the second peak will contain approximately twice as many events (since we have two children for each division), and the third peak contains four times as many observations. Overall, we conclude that our cells reproducibly contain a subpopulation that behaves as predicted by our model for 3:2 coupling, and as in the experiment by Nagoshi et al.[1].

Clustering method 2. For each cell cycle interval, we can obtain a clock period by taking the mean time between all clock peak-to-peak intervals that overlap. Using this clock period and the length of each fully observed cell cycle interval, we can look at the distribution of clock/cell cycle period ratios. We find that in most of our datasets, the cells fall into two groups: one group of cells which couple 1:1, and another group of cells which have a higher mean clock/cell cycle period ratio.

Using Mclust to fit a 1-D Gaussian mixture model to the set of period ratios, we can separate these groups (we restrict the number of clusters to two to avoid overfitting since the ratio data is noisy):

```
data$ratio = data$clockperiod_mean / data$cellcycle_len
m = Mclust(flattened_no_na[, c('ratio')], c(1, 2))
data$classification = m$classification
```

This method enables us to create the plots shown in the bottom row for each dataset in Figures S3, S4 and S5 (see also Table S5: Clock/Cell Cycle Period Ratios and Groups). The first/leftmost figure for each dataset (see also Figure 4a) shows a scatterplot of the clock and cell cycle periods, colored by the classification obtained using the clustering shown above, together with a 75% confidence ellipse for each group[1]. The second plot (in the middle) shows a histogram of the periods and counts for each group. The rightmost plot shows a scatter plot of clock phases at cell division against time similar to the one created for clustering method 1 above, but with different colours: we use the classification by ratio obtained above for colouring the cells.

We observe the following:

- In the unsynchronised populations (Figure S3), the ratios largely fall into the 1:1 group shown in red. The blue group is more scattered and contains cells which 'skip' between stable trajectories on our phase torus.
- In the Dexamethasone-treated cell population at 10% FBS, the clock/cell cycle period ratio of the majority-group of cells has a mean of around 1.1.
- In the Dexamethasone-treated cell populations at 20% FBS (Figures S4b and S5), there are two clearly distinct groups of cells, one with a 1:1, and another one with a 3:2 coupling ratio. Moreover, the colouring by ratio reproduces the clusters obtained by clustering method 1.

[1] The 75% confidence ellipse is estimated from a covariance matrix obtained by fitting a bivariate t-distribution to our data.

Estimation of return phase/Poincaré maps

For each observed cell cycle interval, we can plot the clock phase at its beginning against the clock phase at the end. The result is an approximation of a Poincaré map of the dynamical system of the cell: for each clock phase at which a cell may begin the cell cycle, we can see the preferred phase at the end of the cell cycle. We can make a similar plot for the cell cycle phase: for each complete circadian interval we plot the cell cycle phase at the clock marker peak P_i at the beginning against the cell cycle phase at the time of the clock marker peak P_{i+1} at the end of the interval.

In the case of our unsynchronized datasets (fbs_10 and fbs_15 on the left hand side of Fig. S6c), we can clearly see that the majority of cells prefers to enter/exit at similar locations in our plot, along a fixed point on the main diagonal. In the Dexamethasone-treated conditions, we see a behavior that becomes more different from the unsynchronized case as the period ratio between clock and cell cycle changes from 1:1 towards 4:5.

3. Summary of datasets

3.1 Datasets

We have recorded cells in a variety of conditions to vary the speed of the cell cycle (by means of changing the concentration of FBS), and to perturb the clock (by treating the cells with Dexamethasone to achieve population synchronisation of the clock). A summary of all datasets is shown in Table S1: Summary of Datasets, more details on the data extraction and period lengths are summarized in Table S2: Tracked Cell Counts and Period Lengths.

3.2 Tracking and Dataset Summary

When tracking cells and analysing their clock and cell cycle markers, we obtained good results for cells in 10% and 15% FBS. Clock and cell cycle periods are shown together with an estimate of the standard error of the mean ($\mathrm{sem} = 1.96 \cdot \mathrm{std}(\mathrm{Periods})/\sqrt{n}$).

Note that there is good agreement within the two experiments which were repeated between the two different labs ('fbs_10' and 'fbs_10_r'). Another observation is that in the unsynchronised conditions, clock and cell cycle appear to be running at very similar period lengths (Supplementary Figure S2a). In the Dexamethasone-treated cells, the mean clock period is longer (Supplementary Figure S2a).

As expected, the number of divisions (relative to the number of lineages tracked) is higher in higher concentrations of FBS.

3.3 Data Quality

We show for how many cell cycle intervals we were successfully able to extract the timing of the G1-S transition, and what the average RAE for the clock traces is in each dataset. These numbers can be considered a measure of the quality of the tracking data and our success in extracting information from the resulting time series.

We consider all cell cycle intervals for which we can determine a time of the G1-S transition. In some of these intervals, we may have only been able to match one of the G1 or S/G2/M markers, which will possibly result in a slightly less accurate estimate for the G1-S transition time. We show two success percentages in Table S3: Data Quality for Analysed Cell Cycle Intervals and Clock: in all datasets, we are able to analyse more than 90% of all fully observed cell cycle intervals successfully. When also considering partially observed intervals, this success rate drops to around 50%, since only few partially observed cell cycle intervals have enough data to apply our method (this is not problematic since we can only use fully observed cell cycles in most of our analyses; in most cases, we need to know the duration of the cell cycle interval, which can only be known if it has been observed entirely during our imaging experiment).

Clock RAE values below 0.25 indicate that the clock was functional with a stationary period on average. Only using branches of lineages having an RAE value of less than 0.25 also improves the success rate when analysing the cell cycle. We show a summary of our data quality analysis in Table S3: Data Quality for Analysed Cell Cycle Intervals and Clock.

3.4 Clock vs. Cell Cycle Phase over Time

Dataset fbs_10 and fbs_15:

See Supplementary Movie 2: Cells are unsynchronised, but follow a main trajectory. Some cells 'skip'. G1-arrested cells are shown in grey. Cells for which the clock phase was estimated using peak prediction are shown with a slightly lighter colour.

Dataset dexpulse_fbs_10

See Supplementary Movie 3: We can see that clock and cell cycle are rhythmic. We assign a colour to each group of dividing cells. Cells for which the clock phase was estimated using peak prediction are shown with a slightly lighter colour.

Dataset dexpulse_fbs_20

We did not produce a movie for this dataset, the behaviour is better visualised in the plots from our clustering analysis.

4. Modelling Clock and Cell Cycle as Coupled Oscillators

Differential Equations for Phase. We would like to study clock and cell cycle as a simple stochastic coupled oscillator model with unidirectional coupling. One way to model this is to consider two phase angles $\boldsymbol{\varphi_{cl}}$ and $\boldsymbol{\varphi_{cc}}$ of the clock and cell cycle oscillators which are coupled in one direction, from the clock to the cell cycle.

$$\varphi_{cl}' = v_1 + d\xi$$
$$\varphi_{cc}' = v_2 + famp \cdot Q(\varphi_{cl}, \varphi_{cc}) + d\xi$$

The function $Q(\varphi_{cl}, \varphi_{cc})$ is our gating/coupling function. It describes at which relative phases the clock will be slowing down the cell cycle. We define Q like this, following previous work on the clock for cyanobacteria[14]:

$$Q(\varphi_{cl}, \varphi_{cc}) = -\frac{\left|cos\left(\frac{\varphi_{cl}-\mu_1}{2}\right)\right|^{\alpha}\left|cos\left(\frac{\varphi_{cc}-\mu_2}{2}\right)\right|^{\beta} - \mathcal{N}_0}{1-\mathcal{N}_0}, \text{with}$$

$$\mathcal{N}_0 = \frac{\Gamma(\alpha+1)\Gamma(\beta+1)}{2^{\alpha+\beta}\,\Gamma\left(\frac{\alpha}{2}+1\right)^2\,\Gamma\left(\frac{\beta}{2}+1\right)^2}$$

The normalisation factor $\mathcal{N}_0$ makes function Q integrate to 1 over the range of $[0,2\pi)\times[0,2\pi)$. We may add a white noise term $d\xi$ to simulate molecular noise.

In a deterministic setting (when $d\xi = 0$), we can consider the following scenario: we assume that the clock has a constant forcing period (of, e.g., 24h), and that the cell cycle may phase-couple to this forcing oscillator in different ways, depending on its free-running period (which, in our cell cultures will be dependent upon the amount of growth factor, or the concentration of FBS).

In supplementary Figure S6a (left panel), we can see that φ_{cc} can lock to φ_{cl} due to the forcing term, despite the fact that its natural speed v_2 is slightly faster than that of φ_{cl} (red line). On the bottom, we show Poincaré maps for both phases (see also Figure S6c for their experimental counterparts); intuitively, these show where a trajectory entering at phase φ_{cc} on the left (or φ_{cl} on the bottom, respectively) of a torus plot as shown in S6a will leave on the right (or the top). Points where the resulting curve crosses the main diagonal are fixed points of the system. We see that the 1:1 coupled system has two fixed points for each phase, corresponding to the stable (red) and unstable (blue) trajectory in Figure S6a, left.

In the middle panel, we see the result for coupling with a cell cycle/clock period ratio of 5/4. The system does not lock in a stable fashion (the 5:4 locking region is very small), we see a mixture between the 1:1 and the 3:2 cases with many possible parallel mean trajectories.

The right panel in supplementary Figure S6a shows that the system can also be phase-coupled at a different period ratio – depending on the parameters, we can find coupled

solutions in which we complete three cell cycles every two clock cycles. Each of these coupling regimes would map cell divisions to different (but consistent) clock phases.

Stochastic Simulations When enabling the white noise term $d\xi$, we can simulate the behaviour of our coupled system in settings similar to our experiments. First, we can show that even when noise is present, unsynchronised populations will be phase-coupled (Supplementary Fig. S4b). In this simulation, we choose random starting phases φ_{cl} and φ_{cc} as uniformly random numbers between 0 and 2π. We also fix $\alpha = \beta = 10$, and set $\mu_1 = \mu_2 = \pi$. We use $famp = 2$. We can see that even with white noise, the 1:1 coupling between clock and cell cycle remains stable.

We then looked at reproducing experiments with a 3:2 coupling ratio. This is possible (although the 3:2 coupled region is much smaller than the 1:1 region), and gives results very similar to the experiments (see Figure 6). We observe the following effects:

- We see three peaks in the distribution of all clock phases. This is the result of all peaks in the 2-dimensional density plot for clock phase at division over time 'lining up' at approximately the same phase (left histogram).
- We can also see that the histogram of divisions over time on a population level can look quite random (depending on the number of cells in our sample), since the groups of cells which divide together may overlap due to our simulated noise (right histogram).

We can also reproduce the behaviour we see in our cells with an approximate 5:4 ratio coupling (10% FBS, Dexamethasone treated). Since the 5:4 coupling region is very small in our toy model (it may be larger in a more mechanistic simulation), cells will either fall into the 1:1 and 3:2 coupled regions, depending on the amount of noise. The result is a wider peak in the histogram of clock phases at cell division, and an offset between the peaks in the division-phase density over time (Supplementary Figure S6b, on the right) – therefore, the peaks in this 2-dimensional plot do not line up perfectly anymore, which blurs the distribution of clock phases at cell division (while still allowing a population-level synchronisation of the cell cycle to be clearly visible, see Supplementary Figure S6b, in the middle).

References

1. Nagoshi, E. *et al.* Circadian gene expression in individual fibroblasts: cell-autonomous and self-sustained oscillators pass time to daughter cells. *Cell* **119**, 693-705 (2004).
2. Sakaue-Sawano, A. *et al.* Visualizing spatiotemporal dynamics of multicellular cell-cycle progression. *Cell* **132**, 487-498 (2008).

3. Furler, S., Paterna, J.C., Weibel, M. & Bueler, H. Recombinant AAV vectors containing the foot and mouth disease virus 2A sequence confer efficient bicistronic gene expression in cultured cells and rat substantia nigra neurons. *Gene Ther* **8**, 864-873 (2001).
4. Ryan, M.D. & Drew, J. Foot-and-mouth disease virus 2A oligopeptide mediated cleavage of an artificial polyprotein. *EMBO J* **13**, 928-933 (1994).
5. Albagli-Curiel, O., Lecluse, Y., Pognonec, P., Boulukos, K.E. & Martin, P. A new generation of pPRIG-based retroviral vectors. *BMC Biotechnol* **7**, 85 (2007).
6. Downey, M.J. *et al.* Extracting fluorescent reporter time courses of cell lineages from high-throughput microscopy at low temporal resolution. *PLoS One* **6**, e27886 (2011).
7. Costa, M.J. *et al.* Inference on periodicity of circadian time series. *Biostatistics* (2013).
8. Massey Jr, F.J. The Kolmogorov-Smirnov test for goodness of fit. *J Am Stat Ass* **46**, 68-78 (1951).
9. Mardia, K.V. & Jupp, P.E. *Directional statistics*. (John Willey & sons, 2009).
10. Davison, A.C. & Hinkley, D.V. *Bootstrap methods and their application*. (Cambridge University Press, 1997).
11. Silverman, B.W. *Density estimation for statistics and data analysis*. (Chapman and Hall, 1986).
12. Ihler, A. http://www.ics.uci.edu/~ihler/code/kde.html (2003).
13. Fraley, C. & Raftery, A. http://cran.r-project.org/web/packages/mclust/index.html (2012).
14. Yang, Q., Pando, B.F., Dong, G., Golden, S.S. & van Oudenaarden, A. Circadian gating of the cell cycle revealed in single cyanobacterial cells. *Science* **327**, 1522-1526 (2010).

Supplementary Tables

Table S1: Summary of Datasets

Dataset name	Lab	Condition	Length
fbs_10	Nice	unsynchronised, 10% FBS	72h, 15mins/frame
fbs_10_r	Rotterdam	unsynchronised, 10% FBS	72h, 15mins/frame
fbs_15	Nice	unsynchronised, 15% FBS	72h, 15mins/frame
dexpulse_fbs_10	Rotterdam	Dexamethasone treated, 10% FBS	84h, 30mins/frame
dexpulse_fbs_20	Rotterdam	Dexamethasone treated, 20% FBS	72h, 30mins/frame
dexpulse_fbs_20_2	Rotterdam	Dexamethasone treated, 20% FBS	72h, 15mins/frame

Table S2: Tracked Cell Counts and Period Lengths

Dataset name	Lineages	Divisions	Cell Cycles	Clock Period	Cell Cycle Period
fbs_10	76	173	422	21.9 +/- 1.1 h	21.3 +/- 1.3 h
fbs_15	69	477	1022	19.4 +/- 0.5 h	18.6 +/- 0.6 h
fbs_10_r	31	129	283	21.6 +/- 0.9 h	22.3 +/- 2.2 h
dexpulse_fbs_10	73	380	660	24.2 +/- 0.5 h	20.1 +/- 0.9 h
dexpulse_fbs_20	57	316	677	23.1 +/- 0.9 h	19.1 +/- 0.7 h
dexpulse_fbs_20_2	38	234	487	23.9 +/- 1.4 h	21.3 +/- 1.1 h

Table S3: Data Quality for Analysed Cell Cycle Intervals and Clock

Dataset name	Success	G1/SG2M only	G1 Arrest/No Fit	Mean RAE
fbs_10	261 (97% / 62%)	21 / 25	96 / 161	0.26
fbs_10 *(rae < 0.25)*	150 (96% / 66%)	12 / 12	50 / 76	0.15
fbs_10_r	134 (96% / 47%)	2 / 17	17 / 149	0.24
fbs_10_r *(rae < 0.25)*	100 (96% / 53%)	0 / 13	9 / 88	0.15
fbs_15	583 (100% / 57%)	49 / 51	107 / 439	0.18
fbs_15 *(rae < 0.25)*	452 (99% / 64%)	41 / 31	69 / 258	0.13
dexpulse_fbs_10	409 (98% / 62%)	1 / 89	135 / 251	0.17
dexpulse_fbs_10 *(rae < 0.25)*	392 (99% / 68%)	1 / 85	125 / 185	0.10
dexpulse_fbs_20	368 (94% / 54%)	0 / 64	74 / 309	0.13
dexpulse_fbs_20 *(rae < 0.25)*	315 (94% / 66%)	0 / 57	47 / 164	0.10
dexpulse_fbs_20_2	186 (67% / 38%)	6 / 28	27 / 301	0.25
dexpulse_fbs_20_2 *(rae < 0.25)*	111 (65% / 44%)	4 / 9	12 / 144	0.16

Table S4: Cell Cycle Event Analysis, and background vs. phase distribution test p-values

Dataset name	G1 Length	S/G2/M Length	Mean Division Phase	Mean G1-S Phase
fbs_10	10.5 ± 1.1 h	15.6 ± 1.7 h	3.83 ± 0.25 (**p=0.001**)	0.04 ± 0.24 **(p=0.001)**
fbs_10 *(rae < 0.25)*	10.1 ± 1.3 h	14.6 ± 2.1 h	3.91 ± 0.27 (**p=0.001**)	0.02 ± 0.27 **(p=0.001)**
fbs_10_r	9.5 ± 1.0 h	13.4 ± 1.3 h	3.78 ± 0.35 (**p=0.001**)	5.81 ± 0.33 **(p=0.002)**
fbs_10_r *(rae < 0.25)*	8.9 ± 1.1 h	12.6 ± 1.1 h	3.79 ± 0.36 (**p=0.001**)	5.92 ± 0.34 **(p=0.002)**
fbs_15	8.6 ± 0.4 h	10.2 ± 0.4 h	3.97 ± 0.14 (**p=0.001**)	0.11 ± 0.15 **(p=0.001)**
fbs_15 *(rae < 0.25)*	8.7 ± 0.4 h	9.7 ± 0.3 h	3.99 ± 0.14 (**p=0.001**)	0.12 ± 0.16 **(p=0.001)**
dexpulse_fbs_10	9.5 ± 0.7 h	11.4 ± 0.7 h	3.50 ± 0.44 (**p=0.001**)	6.00 ± 1.02 (p=1.000)
dexpulse_fbs_10 *(rae < 0.25)*	9.5 ± 0.7 h	11.4 ± 0.7 h	3.50 ± 0.44 (**p=0.001**)	6.00 ± 1.02 (p=1.000)
dexpulse_fbs_20	6.5 ± 0.4 h	11.6 ± 0.5 h	3.70 ± 0.24 (**p=0.001**)	6.02 ± 0.29 **(p=0.001)**
dexpulse_fbs_20 *(rae < 0.25)*	6.4 ± 0.5 h	11.9 ± 0.5 h	3.68 ± 0.24 (**p=0.001**)	6.02 ± 0.28 **(p=0.001)**
dexpulse_fbs_20_2	7.6 ± 0.6 h	11.2 ± 0.7 h	3.90 ± 0.64 (**p=0.005**)	0.03 ± 0.47 **(p=0.002)**
dexpulse_fbs_20_2 *(rae < 0.25)*	8.4 ± 0.9 h	11.0 ± 0.9 h	4.01 ± 0.68 (**p=0.020**)	0.10 ± 0.72 **(p=0.020)**

Table S5: Clock/Cell Cycle Period Ratios and Groups

Dataset name	Grp.	# Cell Cycles	Mean Ratio	Clock Median [h]	Clock Std.	Cell Cycle median [h]	Cell Cycle Std.
fbs_10	1	55	1.018	19.62	4.476	19.5	4.14
fbs_10	2	29	1.121	24.25	7.231	20.75	8.09
fbs_15	1	235	0.9989	17.25	3.658	17.5	3.88
fbs_15	2	48	1.307	23.5	5.373	18	6.004
dexpulse_fbs_10	1	152	1.144	22.5	2.891	20	4.757
dexpulse_fbs_10	2	14	2.514	47	11.83	16.25	3.587
dexpulse_fbs_20r	1	97	1.092	21.25	3.51	19.5	4.138
dexpulse_fbs_20r	2	33	1.804	29	6.043	16.5	2.762
dexpulse_fbs_20r2	1	50	0.9991	21.81	2.876	21.75	3.733
dexpulse_fbs_20r2	2	31	1.84	27.25	9.157	16.25	4.451

SUPPLEMENTARY FIGURES LEGEND

Figure S1: the FUCCI-2A system

a, Scheme of the FUCCI-2A construct. CMV pro: CMV promoter; RU5: 5' long terminal repeats (LTR) from MMLV; (gag) - U3: contains CIS viral elements (e.g. Psi); E2-Crimson::Gem (blue): E2-Crimson::Geminin fusion. It is separated from the mKO2::hCdt1 (red) upon translation, through cleavage of the 2A peptide; IRES-puro: puromycin resistance allowing for selection of dual FUCCI positive cells, under control of an IRES. b, Restriction map of the FUCCI-2A transfer plasmid (pPRIPu CrUCCI). c, Cell Cycle analysis in proliferating NIH3T3_Reverbα::Venus-FUCCI-2A cells. Hoechst staining profile and cell fluorescence have been superimposed. P5 area represents cells with a 2C DNA content (G1 or Early S). In P9 area, DNA content progressively increases from 2C to 4C (S phase). In P10 area, cells have a 4C DNA content (G2). As expected, cells that only express mKO2 fluorescence (red) are in G1 and cells that only express E2-Crimson (blue) are in S/G2. Cells that express both markers have a DNA content consistent with "Early S" phase. d, e, and f, Box plot showing *Reverbα* (d), *CcnE2* (e) and *CcnA2* (f) mRNA levels found in cells in different cell cycle phases. Cells were sorted into early G1, G1, early S and S/G2/M based on cell cycle markers. qRT-PCR revealed that *Reverbα* and cyclins expression was as expected (i.e. *Reverbα* peaking in early G1/G1, *CyclinA2* is absent in G1 and *CyclinE2* is expressed in G1 and early S).

Figure S2: Timeseries Analysis Results

a, Clock (blue) and Cell Cycle (red) Period lengths analysis. From left to right: 10% FBS unsynchronised, 15% FBS unsynchronised, 10% Dexamethasone-treated, 20% Dexamethasone-treated, and repeat experiment for 20% Dexamethasone treatment below on the right. b, Phase histograms for G1-S transition, from left to right: 10% FBS unsynchronised, 15% FBS unsynchronised, 10% Dexamethasone-treated. c, Phase histograms for cell divisions, from left to right: 10% FBS unsynchronised, 15% FBS unsynchronised, 10% Dexamethasone-treated. d, Population level analysis of clock peaks (blue/top), cell divisions (red/middle), and G1-S transitions (yellow/bottom) over the course of the experiment. From left to right: 10% FBS unsynchronised, 15% FBS unsynchronised, 10% Dexamethasone-treated. e, Split-population analysis for Clock/Cell Cycle Period ratios of 1:1 and 3:2. On the left: The first/purple histograms show the clock phases at cell division for the 1:1 coupled subpopulation. The second/green histograms show the 3:2 coupled subpopulation. On the right: population-level clock peak and cell division histograms. We show data from two separate experiments in 20% FBS with Dexamethasone treatment

(dexpulse_fbs_20 and dexpulse_fbs_20_2), and the result of combining the datasets on the bottom.

Conditions: fbs_10 = Unsynchronized cells with 10% FBS; fbs_15 = Unsynchronized cells with 15% FBS; dexpulse_fbs_10 = Dex-synchronized cells with 10% FBS, dexpulse_fbs_20 = Dex-synchronized cells with 20% FBS

Figure S3: Cell Division Clustering Analysis for Unsynchronised Cell Populations

We show the results from our two types of clustering for the fbs_10 (subfigure a.) and fbs_15 (subfigure b.) datasets. The top row shows the clusters obtained using 2-D clustering on the clock phase at cell division, and the experiment time. On the left, we show the clusters, on the right, we show the histograms for the clock phase at cell division that correspond to each cluster. Below, we show the clusters obtained when grouping cell cycle intervals by their clock/cell cycle period ratio. We show a scatterplot of clock and cell cycle periods on the left, the resulting period histograms and counts for both groups in the middle, and the resulting clusters on a scatterplot of clock phase at cell division over time on the right. In both cases, the ratio isolates a dominant subgroup of cells which have a 1:1 coupling ratio, and a separate, smaller group of cells which corresponds to stochastic ‘skipping’ behaviour (i.e. cells that move between stable trajectories on the torus due to molecular noise).

Conditions: fbs_10 = Unsynchronized cells with 10% FBS; fbs_15 = Unsynchronized cells with 15% FBS

Figure S4: Cell Division Clustering Analysis for Dexamethasone-treated Cell Populations

We show the results from our two types of clustering for the dexpulse_fbs_10 (subfigure a.) and dexpulse_fbs_20 (subfigure b.) datasets. The top row shows the clusters obtained using 2-D clustering on the clock phase at cell division, and the experiment time. On the left, we show the clusters. On the right, we show the histograms for the clock phase at cell division that correspond to each cluster. Below, we show the clusters obtained when grouping cell cycle intervals by their clock/cell cycle period ratio. We show a scatterplot of clock and cell cycle periods on the left, the resulting period histograms and counts for both groups in the middle, and the resulting clusters on a scatterplot of clock phase at cell division over time on the right.

For 10% FBS, we can see that there may be a small subpopulation that couples at a ratio of > 1.1, and a dominant subpopulation that couples at a ratio of 1:1. The clock phase at cell

division/experiment time clustering shows that clusters of cell divisions exist, however, the transitions between these clusters within the same lineage are not very stable.

For 20% FBS, we clearly see two subpopulations of lineages. On the top, these can be identified as 1) lineages with their first division in the red cluster, and subsequent divisions in the blue and purple clusters (arrows going right, and right), and 2) lineages with their first division in the red cluster and subsequent divisions in the yellow and green clusters (arrows going down and then up). Subgroups of a very similar composition are identified when clustering by clock/cell cycle period ratio.

Conditions: dexpulse_fbs_10 = Dexamethasone-synchronised cells with 10% FBS; dexpulse_fbs_20 = Dexamethasone-synchronised cells with 20% FBS

Figure S5: Cell Division Clustering Analysis for Dexamethasone-treated Cell Populations, repeat experiment

We show the results of a second experiment with Dexamethasone-synchronised cells in 20% FBS. Our findings largely agree with the results shown in Figure S4 b (however, note that the number of tracked cells is significantly lower compared to dataset dexpulse_fbs_20).

Figure S6: Modelling Clock and Cell Cycle as Coupled Oscillators

a, Solutions for the (deterministic) phase differential equations. Left panel: ratio = 1:1, middle panel: ratio = 5:4, right panel: 3:2;

b, Stochastic simulation results for 5:4 coupling;

c. Estimated Poincaré maps from four datasets which were used to inform our modelling. 1:1 coupled subpopulations produce a concentrations of return points around $(\frac{\pi}{2}, \frac{\pi}{2})$, which is where our deterministic model has its stable fixed point.

Figure S7: Estimated vectorfields

Estimated vectorfields/phase diagrams from experimental data for cells in the conditions indicated above each plot. The red dashed curve shows the mean trajectory and the blue levels show the density of cells passing through a region. The arrows show the mean direction that the cells flow in near that point on the torus.

Legends for the supporting videos.

Supplementary Movie 1: Dividing cells cultured in 15% FBS. We overlay the brightfield image with the three channels for the nuclear markers (red: Cdt1:mKO2 / G1 phase, blue: Geminin:E2Crimson / S-G2-M phases, and green: Reverba:Venus / Clock). We can see many cells start transparent or green (corresponding to low/high levels of the clock marker), then turn red during the G1 phase. Many cells will in fact turn yellow (i.e. a mixture of red and green), indicating that the clock marker is at a high level during the G1-S transition. Around the G1-S transition, the red marker drops to near zero, and the blue marker starts rising, reaching its maximum level (making blue or cyan nuclei) just before cell division.

Supplementary Movie 2: Temporal progression of clock and cell cycle phases for unstimulated cells in 15% FBS. We show the clock phase on the horizontal axis, illustrated by a green and black bar on the top which shows the relative clock marker level (high on the sides, low in the middle). The vertical axis shows the progression of the cell cycle. The coloured bar on the right-hand side illustrates the relative levels of the cell cycle markers (black to red in G1, and red to blue in S-G2-M). We also mark G1-S transition and cell division as horizontal yellow lines. Cells are drawn as blue dots (turning grey once they become confluent) which move from the bottom to the top as they progress though the cell cycle, and from the left to the right according to their clock phase (in this diagram measured as the normalized time between two clock peaks). In the background, we show an estimated vector field which indicates the mean direction cells are taking at each point in this phase space. On the sides, we show density estimates for the fraction of cells in in each phase. We see that most cells follow a main stream through the middle of the image, crossing the G1-S transition and cell division lines at a distinct mean clock phase each. Moreover, we observe that some cells skip: they leave the main stream of cells because they progress through the cell cycle phase at a slower speed, and re-join the other cells once they arrive at the main trajectory again. Note that we connect sibling cells by a dashed line when possible.

Supplementary Movie 3: Temporal progression of clock and cell cycle phases for Dex-stimulated cells in 10% FBS. This movie is similar to Supplementary Movie 2, however, we now colour the cells according to their division time. The density histogram on the top shows that cells most cluster around similar clock phases due to the Dex-synchronisation. Also, there is no main stream of cells anymore like in SM2. Rather, cells go through cell division in groups at a wider range of clock phases than in the unstimulated case. Towards the end of the movie, most cells become confluent.

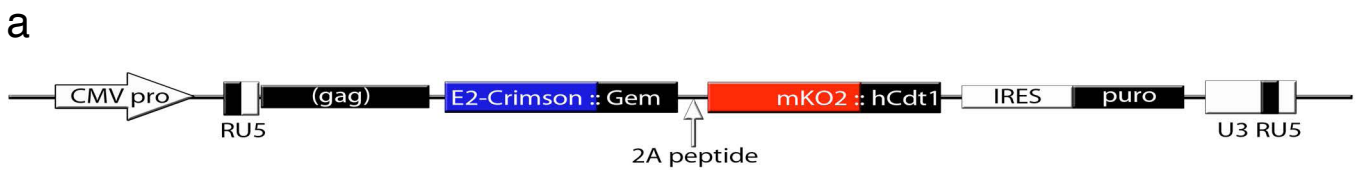

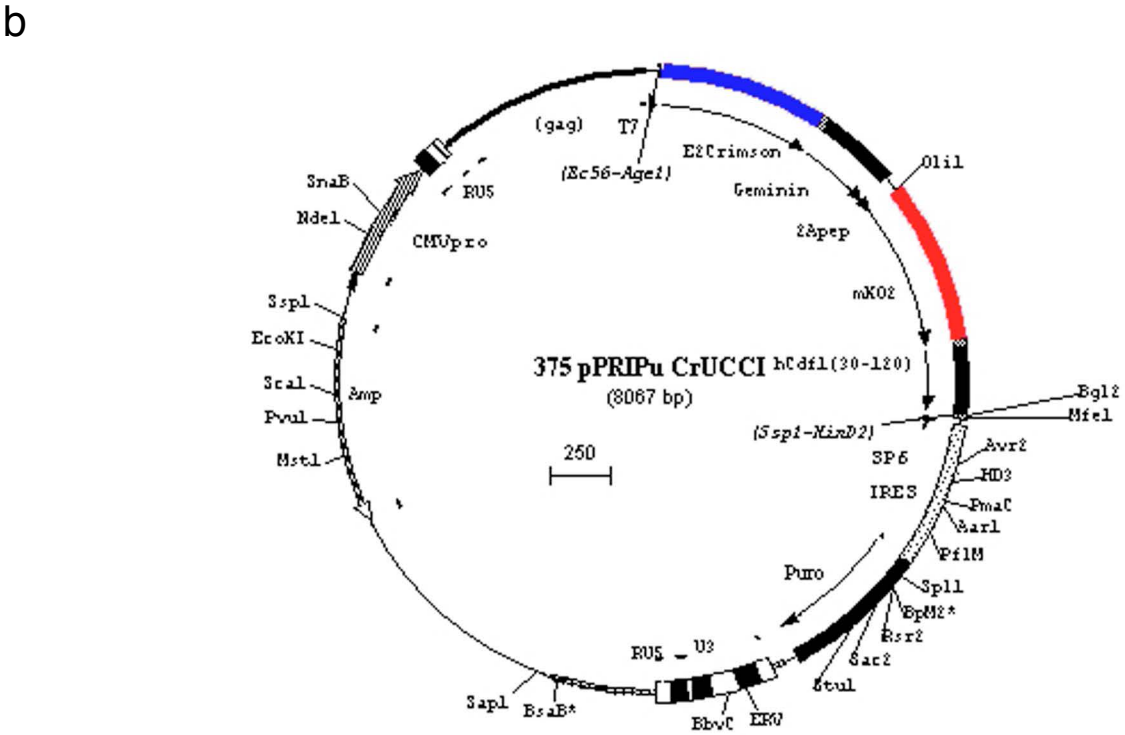

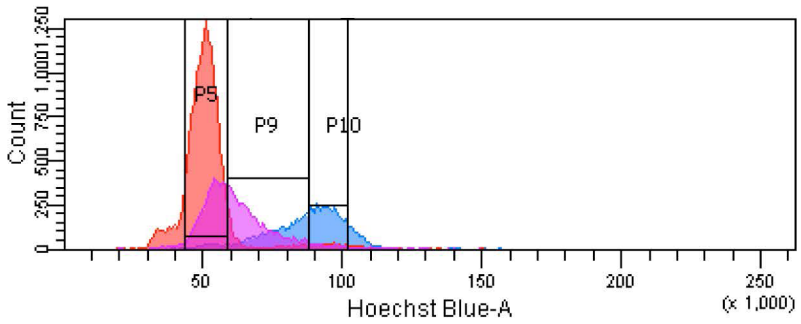

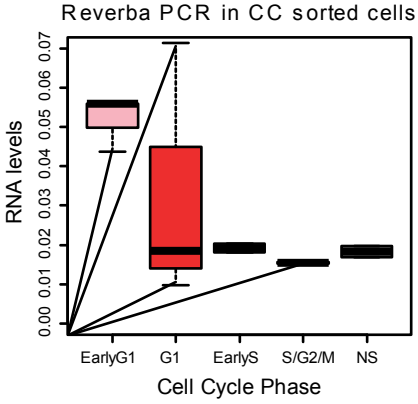

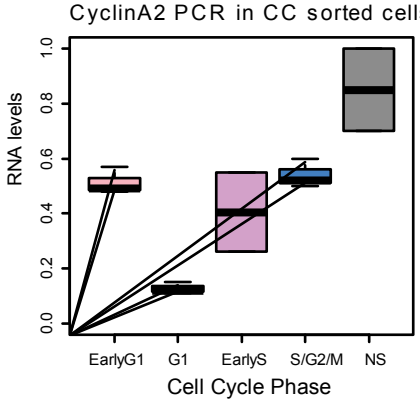

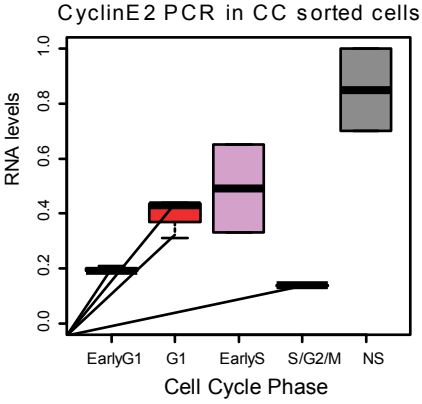

Supplementary-Figure-S1 (Rand)

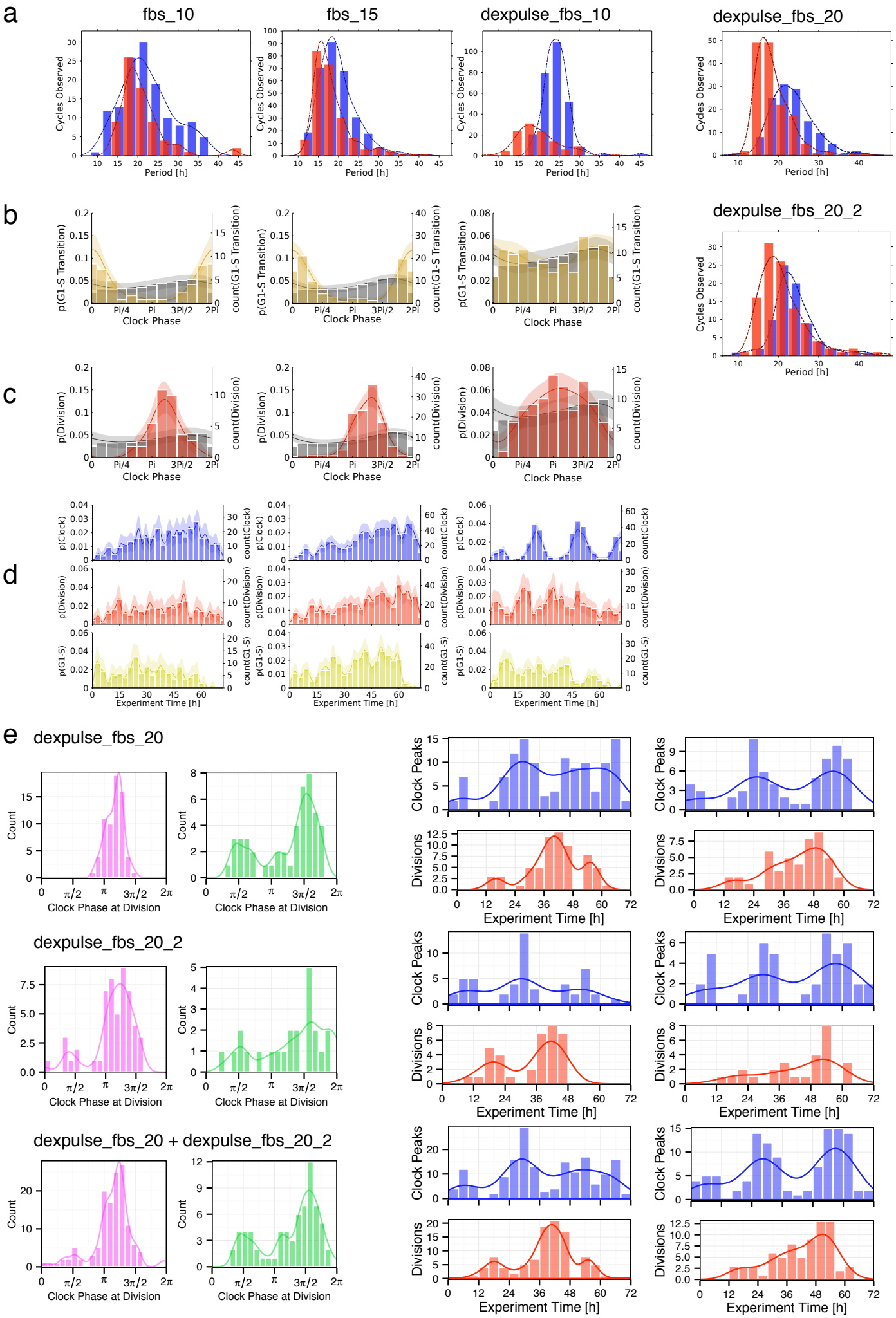

Supplementary-Figure-S2 (Rand)

a Dataset fbs_10: 10% FBS, unsynchronised

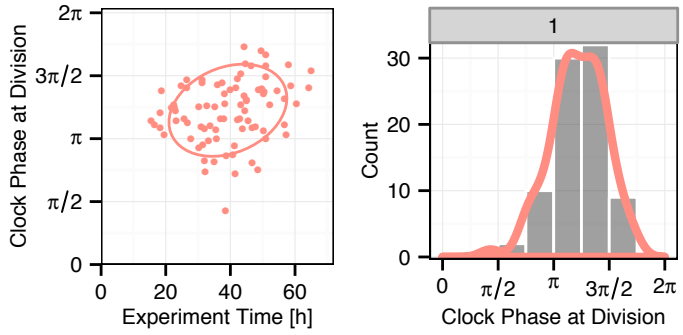

Clustering by clock phase at cell division and time

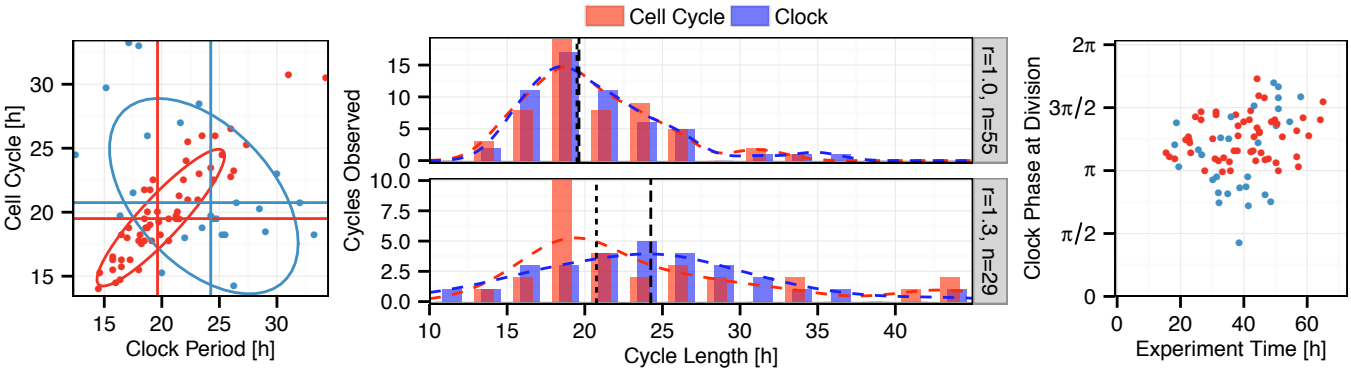

Clustering by clock/cell cycle period ratios

b Dataset fbs_15: 15% FBS, unsynchronised

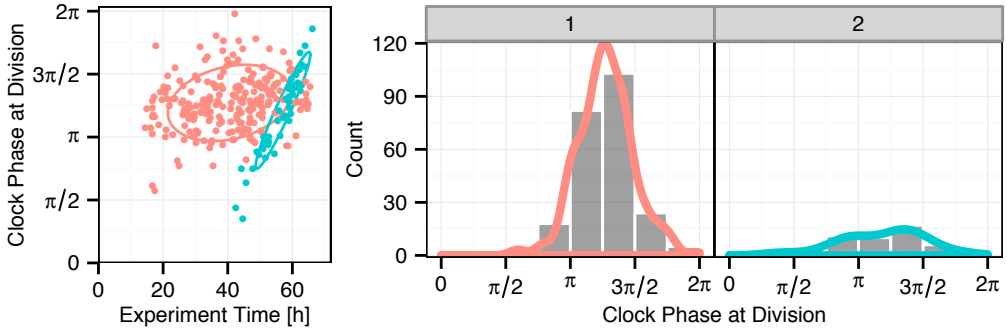

Clustering by clock phase at cell division and time

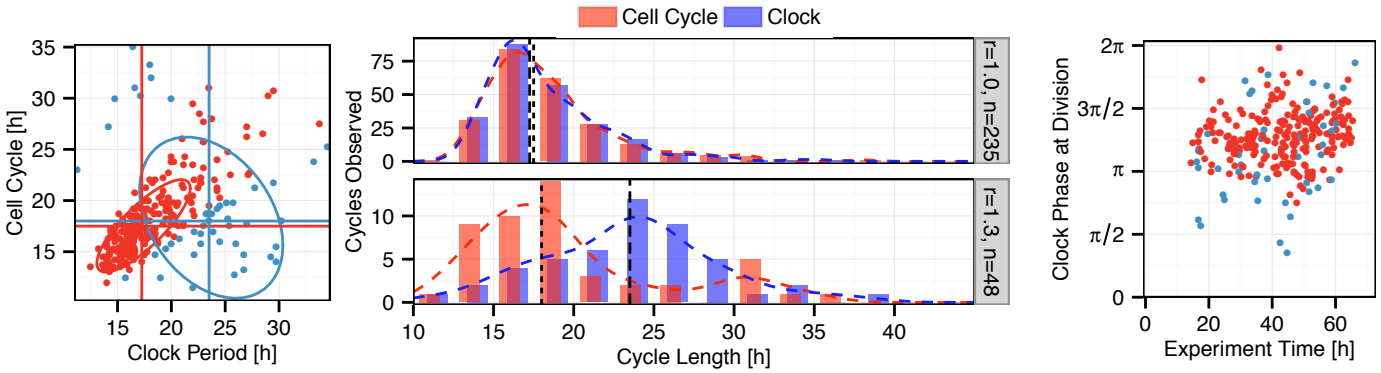

Clustering by clock/cell cycle period ratios

Supplementary-Figure-S3 (Rand)

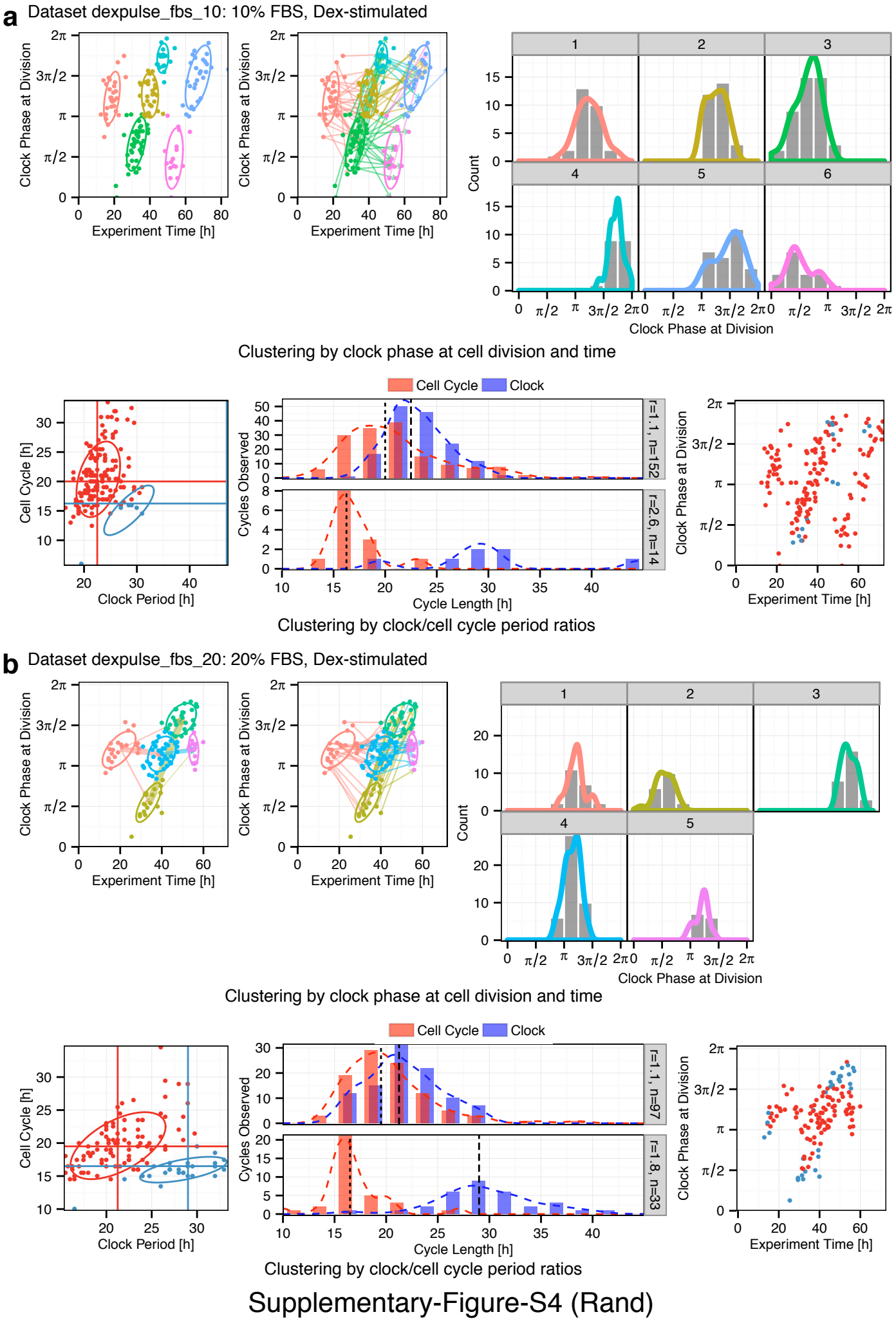

Supplementary-Figure-S4 (Rand)

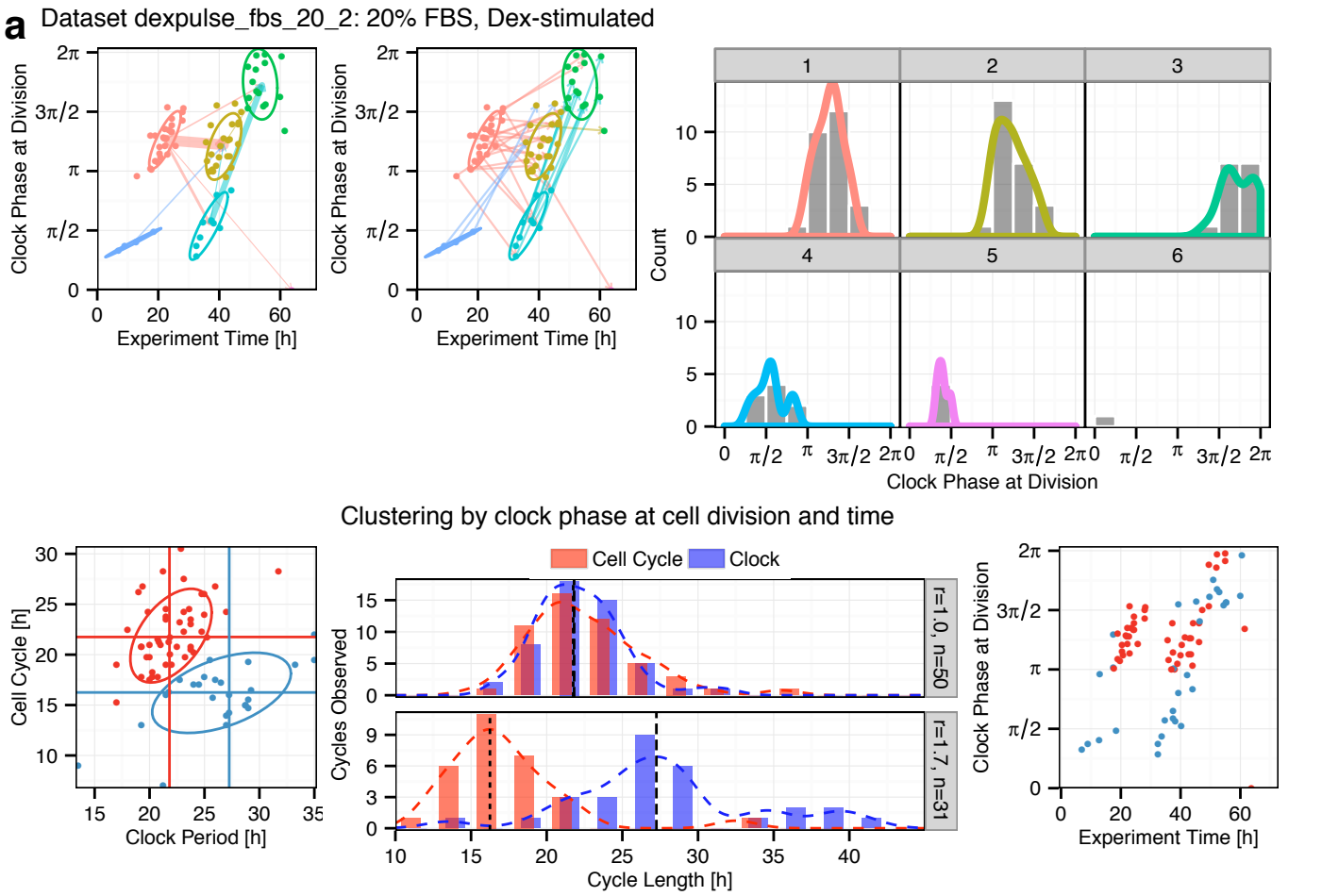

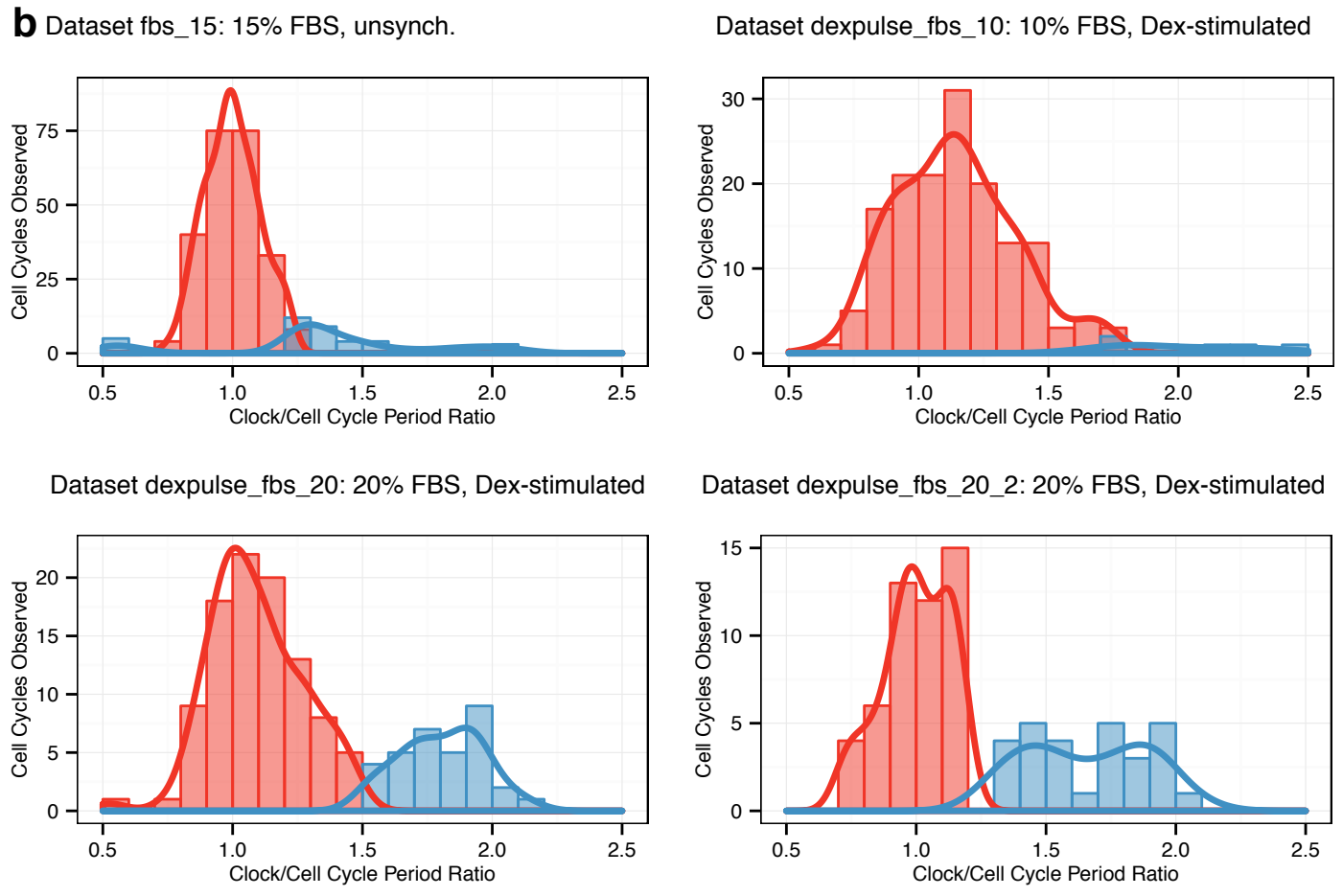

Supplementary-Figure-S5 (Rand)

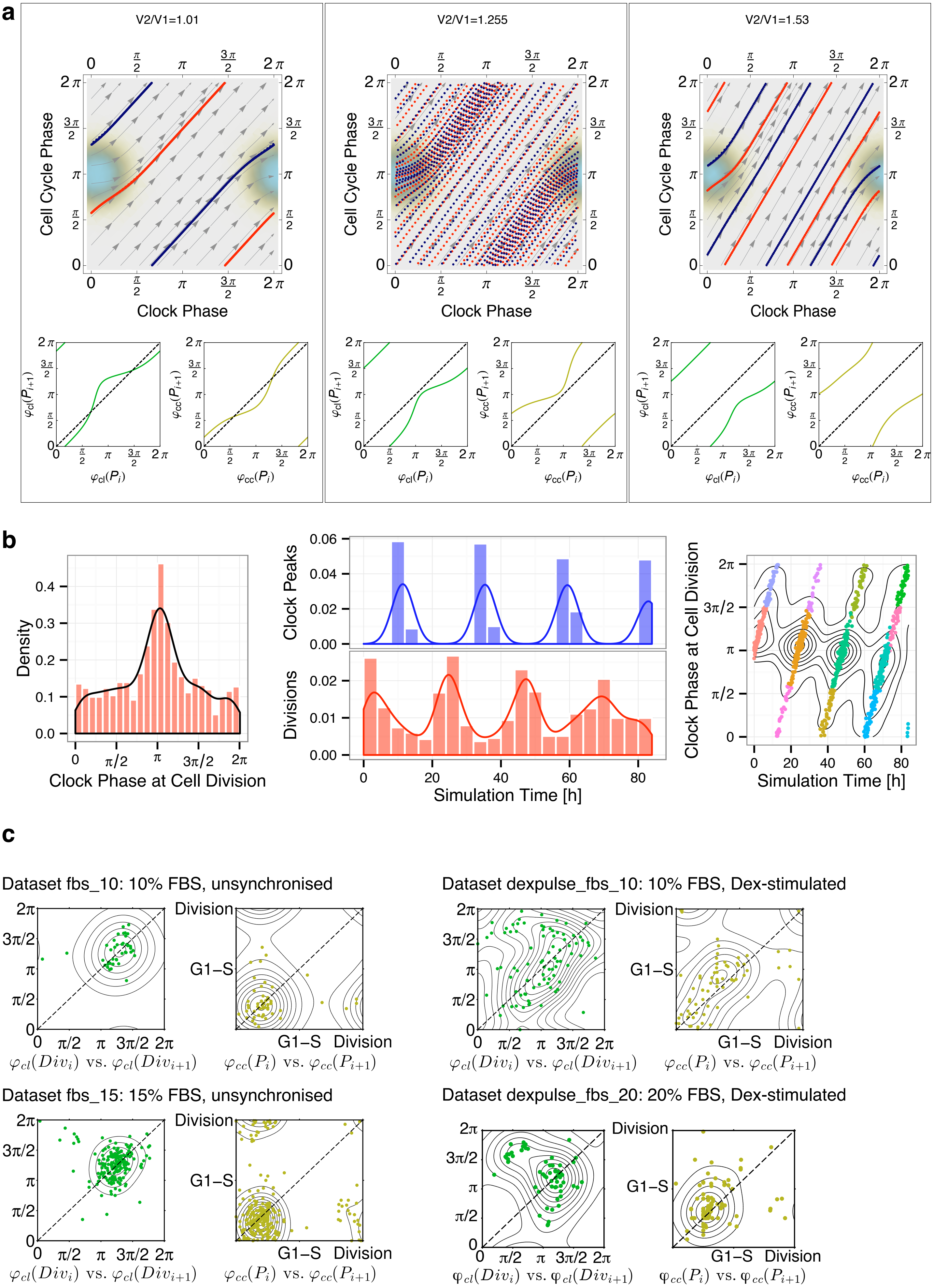

Supplementary-Figure-6 (Rand)

a Dataset fbs_10: 10% FBS, unsynchronised

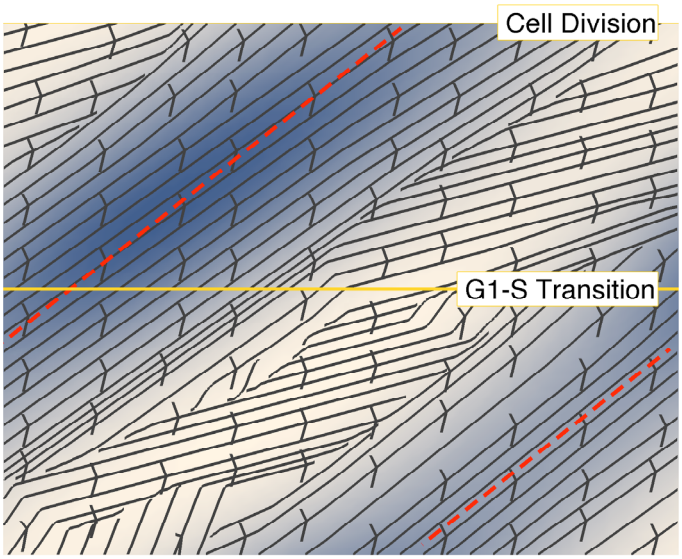

b Dataset fbs_15: 15% FBS, unsynchronised

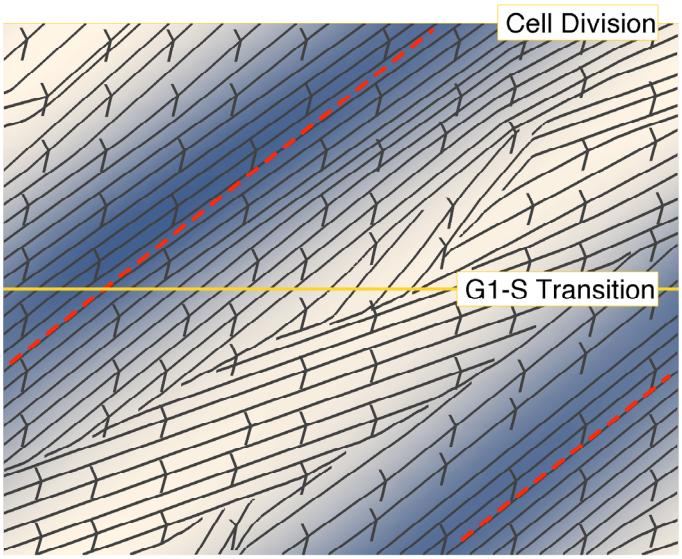

c Dataset dexpulse_fbs_10: 10% FBS, Dex-stimulated

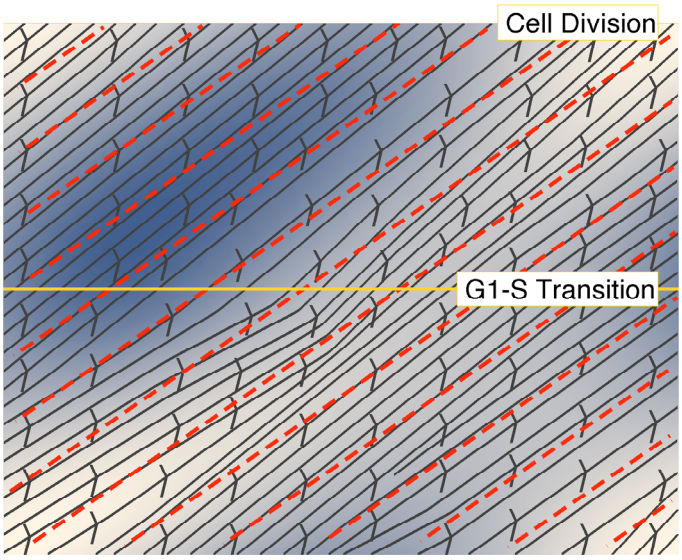

d Dataset dexpulse_fbs_20: 20% FBS, Dex-stimulated

Cells with 1:1 ratio

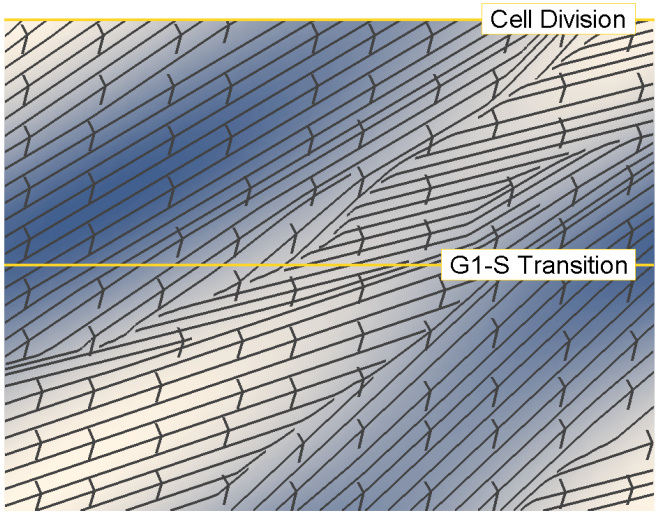

Cells with 3:2 ratio

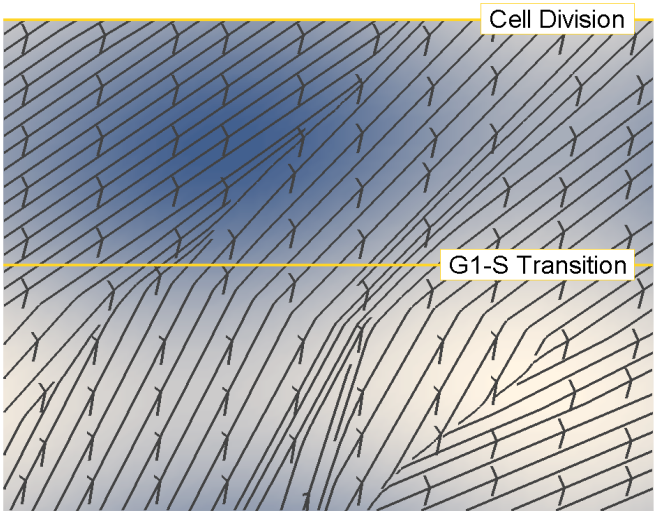

Supplementary-Figure-7 (Rand)